

Analysis and calculation of LR circuit mathematical model for high temperature superconducting induction motor



Bin Liu^{a,*}, Shengjie Wang^a, Bin Zhao^a, Jin Fang^b, Xiaojun Wang^a

^a Beijing Mechanical Equipment Institute, 100854, China

^b School of Electrical Engineering, Beijing Jiaotong University, Beijing, 100044, China

ARTICLE INFO

Keywords:

HTS induction motor
LR circuit
Euler method
Power-law

ABSTRACT

The use of nonlinear superconducting material in high temperature superconducting (HTS) induction motor leads to the problem of accuracy of traditional motor vector analysis method, the electromagnetic mechanism of HTS induction motor is studied by numerical solution of the differential equation of LR circuit in this paper. According to the electromagnetic constitutive relationship of HTS material, the variation law of resistivity of HTS materials is revealed. Combined with the E-J rule of superconducting material, the LR form ordinary material equation of stator current and rotor current is deduced, and the differential equations are discretized by Euler method differential equation. The discrete form of stator current rotor current of motor is finally obtained. Based on the Power-Law principle, the rotor resistant expression of HTS Induction Motor with HTS rotor and the armature resistant expression of HTS Induction Motor with HTS Armature are derived. And the electromagnetic characteristics and operational performances of HTS induction motor with HTS rotor, HTS induction motor with HTS armature and fully superconducting HTS induction motor are discussed respectively. The results show that the ratio of rotor current peak value to superconducting critical current is greater than 1 for both HTS induction motor with HTS rotor and fully superconducting HTS induction motor, and there is a risk of superconducting quench.

1. Introduction

SINCE entering the new century, people's pursuit of environmental protection and efficiency of transportation has become more and more high. At the same time, faced with the double pressure of environment and energy, countries all over the world are looking for better solutions, hoping that electricity can replace other forms of secondary energy. The application of superconducting material can not only reduce the quality and volume of power equipment, but also improve the efficiency of the same capacity motor and enhance environmental adaptability [1–6]. Especially the HTS motor developed by liquid nitrogen cooling is a major solution in the development and application of national energy, information and military technology. Compared with the traditional equipment of the same power, the HTS motor has the advantages of small volume, light weight, high power density and low maintenance cost, and can be widely used in many fields such as ship propulsion, wind power generation, magnetic levitation and flywheel energy storage, which has important academic research value and economic application prospect, and has become the research hotspot of many

research institutions [7–14].

It is well known that HTS materials are nonlinear materials [15], and when designing superconducting motors, superconducting materials are often simply equivalent to copper materials for simulation calculations. This is contrary to the principle of superconducting materials, so the accuracy of calculation is questionable. Based on the application position of superconducting magnets in HTS induction motor, the HTS induction motor is divided into three types, namely HTS induction motor with HTS rotor, HTS induction motor with HTS armature and fully superconducting HTS induction motor respectively. For these three types with considering the characteristics of superconducting materials themselves, the performance of HTS induction motor is studied based on the numerical solution of differential equation of LR circuit, which provides a new idea for the performance analysis of HTS motor.

2. HTS magnet resistivity

The difference of materials used in stator and rotor windings of

This work was supported by National Key R&D Program of China (No: 2016YFB0401504) and China Postdoctoral Science Foundation.

* Corresponding author.

E-mail addresses: 14117396@bjtu.edu.cn (B. Liu), fangseer1@sina.com (J. Fang).

<https://doi.org/10.1016/j.physc.2019.1353579>

Received 24 July 2019; Received in revised form 11 November 2019; Accepted 22 November 2019

Available online 22 November 2019

0921-4534/ © 2019 Elsevier B.V. All rights reserved.

Table 1
Technological parameters of HTS tape used in the dissertation.

Width of tapes [mm]	4.8
Thickness of tapes [mm]	0.18
Thickness of layer [μm]	1
Critical current (self-field, 77K) [A]	140
Minimum bending radius[mm]	30
Maximum rated tensile stress [Mpa]	150
Maximum Tensile Strain Rate	0.25%
Tape insulation	FCR 2/3stack
Interturn withstand voltage [V]	5000
Magnetism	Yes

motors is the reason for the essential difference between HTS motors and traditional motors. Therefore, the first step in designing HTS motors is to understand the electromagnetic characteristics of HTS tapes. In this paper, the main technical parameters of HTS tapes used in HTS motors are shown in Table 1.

Equivalent resistivity expressions of high temperature superconductors can be deduced according to the Power-Law law.

$$\rho_{HTS} = \frac{E_c}{J_c(B)} \left| \frac{J}{J_c(B)} \right|^{n(B)-1} \quad (1)$$

where, E_c is $1\mu\text{V}/\text{cm}$ and $J_c(B)$ is the critical current density considering the dependence of magnetic field.

$$J_c(B) = \frac{J_{c0}}{(1 + B/B_0)^n} \quad (2)$$

According to the Eqs. (1) and (2), the resistivity curves of superconductors under different background magnetic fields can be calculated. The curves of resistivity versus current density are shown in Fig. 1.

From Fig. 1, it can be seen that superconductors have almost no resistivity when their critical current density is much lower than their critical current density. However, with the increase of the current density, the resistance of the superconductor increases. That is to say, the closer to the critical current density, the more obvious the resistance of the superconductor is. When the superconductor enters the current only in the self-field, the resistivity of the superconductor is only $5.53 \times 10^{-13}\Omega\cdot\text{m}$ near the critical current density, which is almost negligible. In addition, it can be seen that the resistivity of superconductors increases with the increase of background magnetic field. When the background magnetic field exceeds a certain value, the resistivity of superconductors should be considered.

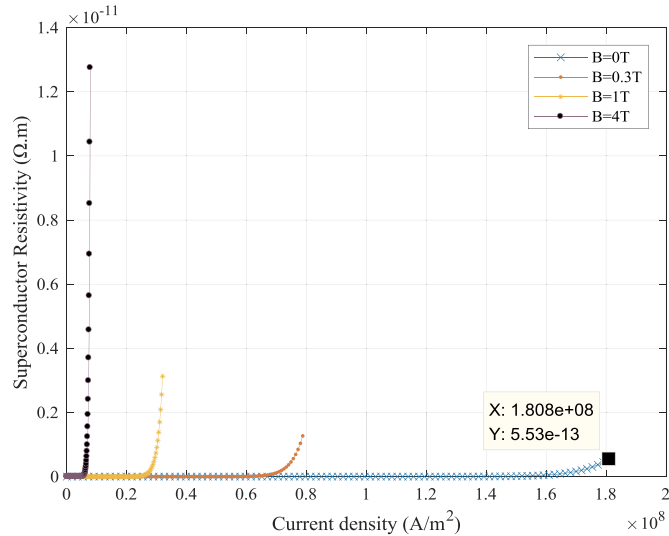


Fig. 1. Change curves of resistivity under different background field.

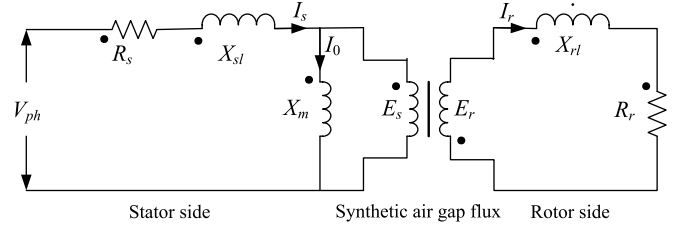


Fig. 2. No converted motor equivalent circuit.

3. LR circuit model of HTS induction motor

According to the application position of superconducting magnets in HTS induction motors, HTS induction motors are divided into three types: HTS induction motor with HTS rotor, HTS induction motor with HTS armature and fully superconducting HTS induction motor. For these three types, the performance of HTS induction motors is studied based on the differential equation numerical solution of LR circuit.

Assume that the terminal voltage of induction motor is V_{ph} , the resistance of stator winding is R_s , the leakage inductance of stator winding is X_{sl} , the excitation inductance is X_m , the leakage inductance of rotor is X_{rl} , the phase resistance of rotor is R_r , the phase current of stator is I_s , the phase current of rotor is I_r , and the excitation current is I_0 . Only excitation inductance is considered, and the effect of excitation impedance is neglected. As a result, the rotor part does not calculate the equivalent circuit diagram of the induction motor to the stator side, as shown in Fig. 2 [16]

When the stator winding of induction motor is passed into three-phase alternating current, the alternating magnetic field will be generated in the air gap. Thus the electromotive force will be generated in the stator winding and the rotor winding, and the power between the stator and the rotor will be transmitted through the air gap to synthesize the flux.

According to the traditional vector method, the equivalent circuit equation of induction motor can be listed.

$$\dot{V}_{ph} = -\dot{E}_s + \dot{I}_s(R_s + jX_{sl}) \quad (3)$$

$$-\dot{E}_s = \dot{I}_0 jX_m \quad (4)$$

$$\dot{E}_r = \frac{s}{k_e} \dot{E}_s \quad (5)$$

$$0 = -\dot{E}_r + \dot{I}_r(R_r + jsX_{rl}) \quad (6)$$

$$\dot{I}_s + \frac{\dot{I}_r}{k_i} = \dot{I}_0 \quad (7)$$

where, k_e is the conversion voltage ratio and k_i is the conversion current ratio.

The analysis of equivalent circuit of induction motor above is calculated based on vector form. For traditional induction motor, the circuit is basically composed of linear components, and the current and voltage waveform is sinusoidal. Therefore, vector analysis method can be used to solve the problem, which is simple and feasible. However, in superconducting induction motors, the superconducting material is a non-linear element, and the current waveform in the circuit may not be sinusoidal. Therefore, the feasibility and accuracy of using vector analysis method to solve the circuit of superconducting induction motor are doubtful. In order to avoid this problem, a differential equation is proposed to study HTS induction motors in this paper.

All vector-form equations of (3)–(7) are transformed into function forms with time.

$$\begin{cases} V_{ph}(t) = -E_s(t) + I_s(t)R_s + L_{\sigma_s} \frac{dI_s(t)}{dt} \end{cases} \quad (8)$$

$$\begin{cases} -E_s(t) = L_m \frac{dI_0(t)}{dt} \end{cases} \quad (9)$$

$$\begin{cases} E_r(t) = \frac{s}{k_e} E_s(t) \end{cases} \quad (10)$$

$$\begin{cases} 0 = -E_r(t) + I_r(t)R_r + sL_{\sigma r} \frac{dI_r(t)}{dt} \end{cases} \quad (11)$$

$$\begin{cases} I_s(t) + \frac{1}{k_i} I_r(t) = I_0(t) \end{cases} \quad (12)$$

By solving the above state equations, the ordinary differential equations of stator current $I_s(t)$ and rotor current $I_r(t)$ can be obtained.

$$\frac{dI_s(t)}{dt} = \frac{\left(\frac{sL_m}{k_e k_i} + sL_{\sigma r}\right)V_{ph}(t) - \left(\frac{sL_m}{k_e k_i} + sL_r\right)R_s I_s(t) + \frac{L_m}{k_i} R_r I_r(t)}{\frac{sL_m L_s}{k_e k_i} + sL_m L_{\sigma r} + sL_{\sigma s} L_{\sigma r}} \quad (13)$$

$$\frac{dI_r(t)}{dt} = \frac{-\frac{sL_m}{k_e} V_{ph}(t) + \frac{sL_m}{k_e} R_s I_s(t) - (L_m + L_{\sigma s})R_r I_r(t)}{\frac{sL_m L_{\sigma s}}{k_e k_i} + sL_m L_{\sigma r} + sL_{\sigma s} L_{\sigma r}} \quad (14)$$

For Eq. (13) and (14), we use Euler method to solve ordinary differential equations to discretize the above differential equations. After discretization, the stator current I_s and rotor current I_r can be easily solved. In order to facilitate better expression, it is assumed that the time step of the solution is h and the time range of the solution is from $t_0 - t_n$. So the number of solutions N can be expressed:

$$N = \frac{t_n - t_0}{h} \quad (15)$$

Therefore, the differential form of stator current I_s and rotor current I_r can be assumed to be the following expression.

$$\frac{dI_s(t)}{dt} = f_1(I_s(t), I_r(t), t) \quad (16)$$

$$\frac{dI_r(t)}{dt} = f_2(I_s(t), I_r(t), t) \quad (17)$$

The following expressions can be obtained by discretizing the above fractal equations of stator current I_s and rotor current I_r .

$$I_s(t_n) = I_s(t_{n-1}) + hf(I_s(t_{n-1}), I_r(t_{n-1}), t_{n-1}) \quad (18)$$

$$I_r(t_n) = I_r(t_{n-1}) + hf(I_s(t_{n-1}), I_r(t_{n-1}), t_{n-1}) \quad (19)$$

The initial conditions are: $I_s(0) = 0$, $I_r(0) = 0$

According to the above results, as long as the terminal voltage $V_{ph}(t)$ of the motor is given, the numerical solution of the stator current and rotor current can be obtained. Thus the power equation and the torque equation of the induction motor can be solved, and the operation performance of the motor can be further analyzed.

3.1. LR circuit model of HTS induction motor with HTS rotor

By replacing the traditional squirrel cage rotor with the HTS squirrel cage rotor, the HTS induction motor with HTS rotor can be obtained. The stator windings are made of three-phase constant conductive material, and the rotor bars are composed of superconducting material. However, the rotor slots should be made into a structure suitable for rectangular superconducting tape. The end ring at both ends of the bars also consists of superconducting material.

Traditional squirrel cage rotors are made of metal materials, and their resistance is approximately constant. In this paper, superconducting materials belong to non-linear components, and their equivalent resistance is in the form of power exponent. Because the properties of superconducting materials are complex, we simplify them as follows:

- (1) The equivalent resistance of HTS squirrel cage conductor always conforms to the power exponential law.
- (2) The end ring of the rotor never fails to quench.
- (3) Regardless of the influence of magnetic field on the critical current, it is regarded as a material with a single critical current I_c .
- (4) Without considering the current distribution of the rotor superconducting bars, the current distribution is considered to be uniform.
- (5) The cooling structure of superconducting materials in motors is also not considered.

Assuming that the equivalent length of each phase of a squirrel cage superconducting rotor is l_r , the equivalent resistance of each phase of the superconducting rotor can be expressed as follows:

$$R_r = \frac{E_{r0}}{I_c} \left| \frac{I_r}{I_c} \right|^{n-1} \quad (20)$$

where, $E_{r0} = E_c l_r$, I_c is the critical current of superconducting materials (77K, liquid nitrogen).

According to formula (20), we can see that the resistance value of the superconducting rotor is mainly affected by the superconducting critical current, the input current of the rotor and the value of n . The existing basic electromagnetic structure parameters of the motor are taken as the analysis model, as shown in Table 2. Based on the above LR differential equation numerical solution, the corresponding rotor resistance is replaced by the equivalent HTS resistance expression in formula (20). The electromagnetic characteristics and operation performance of the HTS induction motor with HTS rotor under the different parameters are researched.

Assuming that the motor runs at 100 Hz, and the critical current of superconducting materials is measured at 77 K liquid nitrogen. Here n is taken as 21. By changing the critical current value of the superconducting rotor, the electromagnetic torque and peak rotor current of the HTS induction motor with HTS rotor with different critical currents can be obtained.

The stator winding of superconducting motor adopts Y connection method, the motor terminal voltage V_{ph} can be expressed as:

$$V_{ph}(t) = \frac{500\sqrt{2}}{\sqrt{3}} \sin(2\pi ft) \quad (21)$$

Firstly, the rotor current curve of superconducting motor under rated operating conditions is calculated, as shown in Fig. 3. It can be seen from the figure that the rotor current waveform of the superconducting motor is not sinusoidal at this time, and there is a constant value at the peak for a long time, which may be due to the results of the non-linear characteristics of the superconducting material itself.

Fig. 4 shows the relationship between electromagnetic torque and slip rate of HTS induction motor with HTS rotor with different critical current. Here, different critical currents refer to values at different operating temperatures, and subsequent chapters on critical currents are also studied at different operating temperatures. It can be seen from the figure that the electromagnetic torque increases with the increase of critical current I_c . However, before the synchronization speed is

Table 2
Rated electromagnetic parameters of designed motor

Rated power[kW]	100
Rated voltage[V]	500
Rated frequency[Hz]	100
Stator core out diameter [mm]	345
Stator core inner diameter[mm]	170
Outer diameter of rotor core[mm]	159
Core length[mm]	200
Stator leakage reactance[Ω]	0.428
Rotor leakage reactance[Ω]	0.136
Excitation reactance[Ω]	2.022

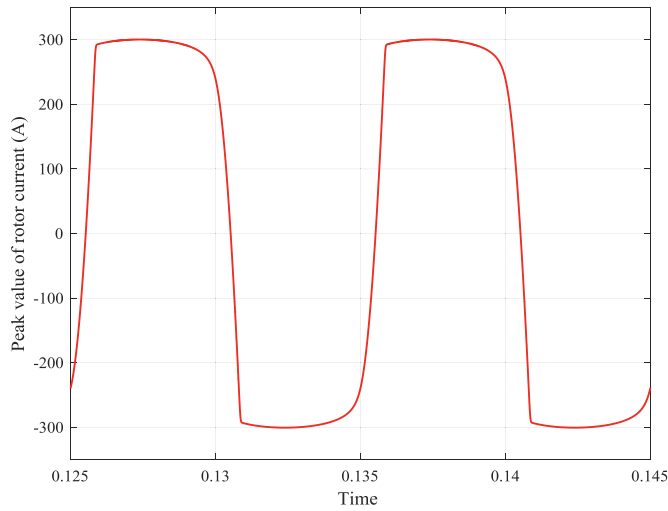


Fig. 3. Rotor current waveform curve with rated condition.

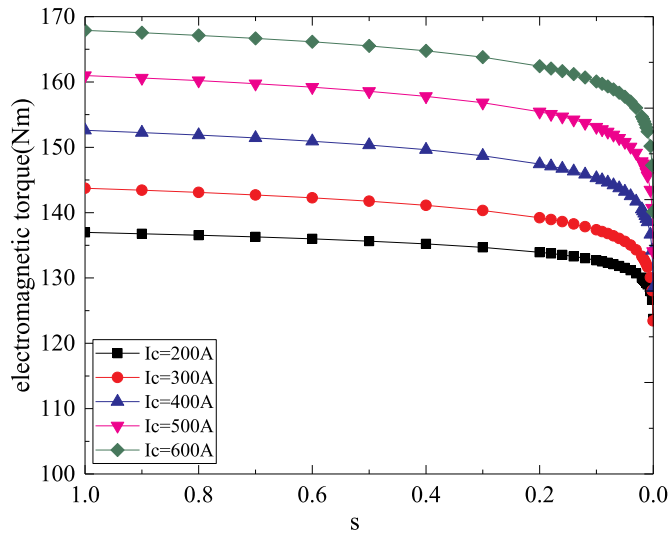


Fig. 4. Electromagnetic torque vs the slip rate under different critical currents with HTS rotor.

reached, the maximum torque is almost unchanged, and the starting torque is the largest. This effect brings convenience to the control of superconducting motor.

Although the electromagnetic torque of the superconducting induction motor remains almost unchanged, it also brings other problems. Fig. 5 shows the ratio of peak current to critical current under different critical current conditions. It can be seen that although the critical current is different, the ratio of rotor current to critical current is very close. According to the equivalent resistance formula (20), the approximation of this ratio means that the equivalent resistance is close, which also means that the ratio of the rotor equivalent resistance to the rotor leakage reactance is almost constant. However, it can be seen from the figure that the ratio of the peak current to the critical current of the rotor is very high, up to 1.7 times. Even when the motor reaches the rated state, the ratio of the peak current to the critical current of the rotor is still greater than 1. In this case, whether the superconducting material can maintain thermal stability under cooling condition, and the equivalent resistance formula can still maintain the power exponential relationship, these need to be further explored. Moreover, the rotor current is the largest when the superconducting motor starts. With the increase of the motor speed, the current carrying capacity of the superconducting material decreases gradually. Although

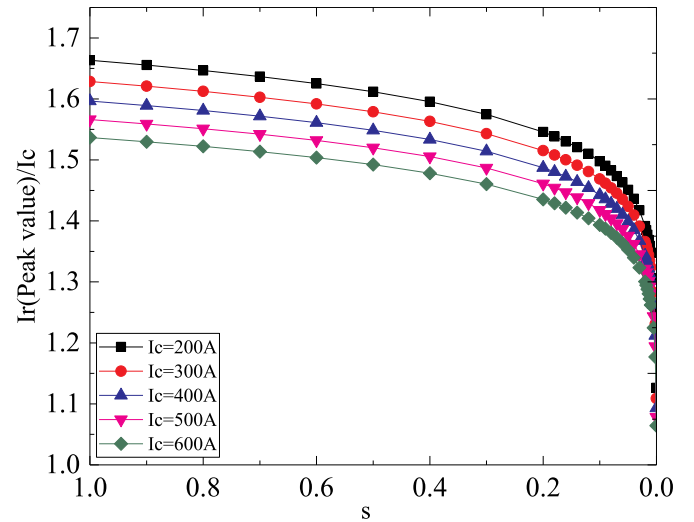


Fig. 5. Ratio of peak current of rotor to critical current vs slip rate under different critical current.

this kind of motor has great advantages, engineers should consider the risk of superconducting material quenching when designing HTS induction motor with HTS rotor. In addition, the critical current value of superconducting materials required is too large. For practical superconducting materials, it is also affected by factors such as external magnetic field, ambient temperature, mechanical stress and so on. The critical current value may be further reduced.

3.2. LR circuit model of HTS induction motor with HTS armature

The biggest difference between HTS induction motor with HTS armature and traditional induction motor is the material of stator winding. Because HTS material is oxide ceramic material, it is brittle and has poor mechanical performance. When the mechanical stress (such as tensile stress, bending stress, etc.) reaches a certain limit, the critical current of the superconducting material will drop sharply, and cannot bend arbitrarily like copper wire. Therefore, the stator superconducting windings will generally be made into runaway coils [17].

In this paper, in order to simplify the complexity of superconducting materials, the influence of external magnetic field on the critical current of superconducting materials is still neglected. Based on the analysis of the parameters of the superconducting motor in Table 2, it is assumed that the total length of the superconducting tape used in a superconducting coil in this paper is L_{coil} , so the resistance of each phase of the superconducting stator winding can be expressed as follows:

$$R_s = \frac{E_{s0}}{aN_s^2 I_c} \left| \frac{I_s}{aN_s I_c} \right|^{n-1} \quad (22)$$

where, $E_{s0} = E_c L_{coil}$, a is the number of parallel branches, N_s is the number of wires per conductor.

Firstly, according to the design parameters of superconducting motor, the curves of armature current and rotor current under rated state are calculated, as shown in Figs. 6 and 7. From the two figures, it can be seen that although the superconducting material is a non-linear material, the stator superconducting armature current and rotor current still maintain a sinusoidal curve state, that is to say, the traditional motor control strategy is still applicable to this type of superconducting motor.

Fig. 8 shows the variation curve between the peak value of stator superconducting armature current and slip rate under different frequency and critical current of superconducting tape for HTS induction motor with HTS armature. It can be seen from the figure that the peak armature current of HTS induction motor with HTS armature is almost

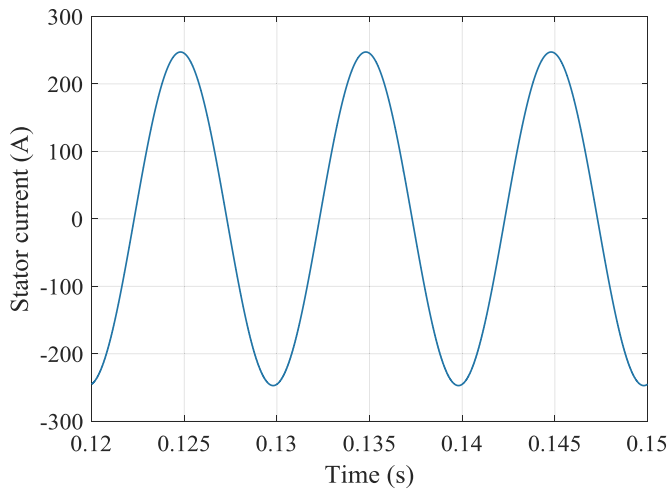


Fig. 6. Variation curve of stator current.

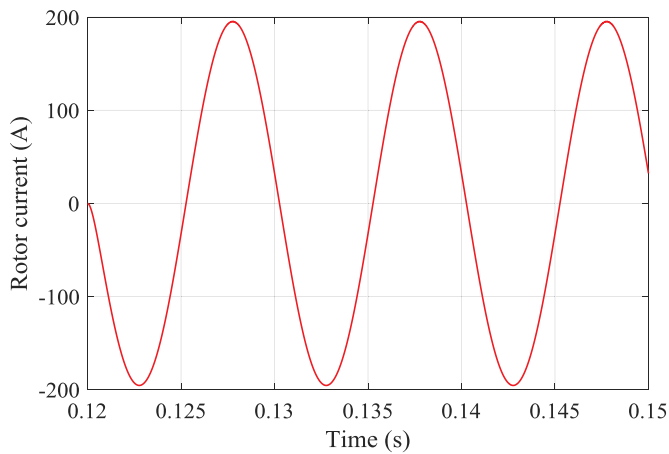


Fig. 7. Variation curve of rotor current.

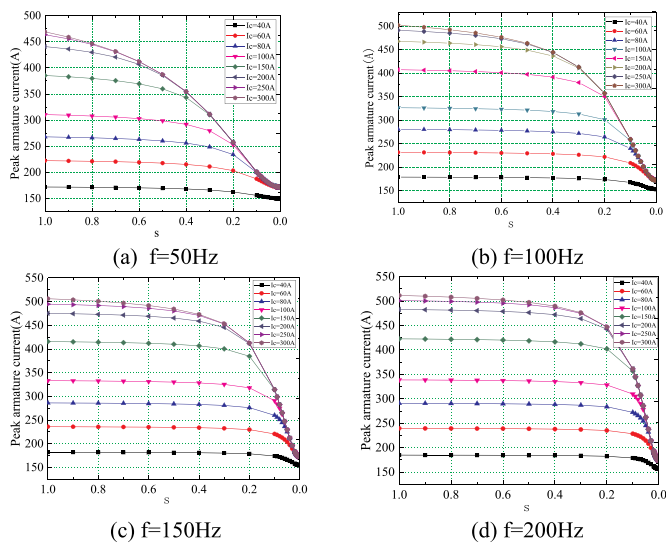


Fig. 8. Armature current vs slip rate under different critical currents.

unchanged in a large range of operation, that is, the range of speed regulation is wide under the condition of lower critical current. Because in this paper, the superconducting coil adopts two parallel paths, double-layer winding method, it can be observed that when the critical current of the superconducting tape increases from 40A to 300A, the

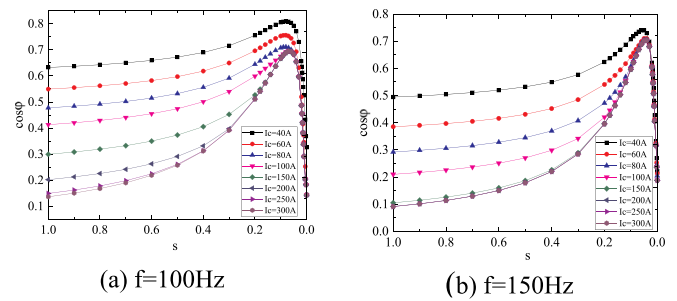


Fig. 9. Power factor vs slip rate under different critical currents.

peak armature current is lower than the critical current value of the superconducting coil. With the increase of frequency from 50Hz to 200Hz, the peak value of armature current becomes more and more flat in a large range. This is because the increase of critical current gives the superconducting armature winding greater margin, and the peak value of armature current is much lower than the critical current of superconducting coil.

Fig. 9 shows the change curve between the power factor and slip rate of superconducting induction motor under different frequency and critical current of superconducting tape. From the figure, it can be seen that the power factor of superconducting motor increases with the increase of motor speed before the rated point, but decreases when it exceeds the rated point. Moreover, when the critical current of superconducting tape increases from 40A to 300A, the power factor decreases. When the critical current increases to a certain value, especially from 250A to 300A, the power factor remains basically unchanged.

The speed of transition from superconducting state to normal state of HTS materials is expressed by n value, so n value is also an important performance parameter of superconducting materials. According to the rated parameters of the superconducting motor, the critical current of the superconducting tape is set to 80A. The influence of the superconducting n value on the power factor is calculated, as shown in Fig. 10. It can be seen from the graph that the power factor increases with the increase of n value, but when n value is between 20 and 100, the increase of power factor is not particularly obvious.

In order to further study the effect of n value on the performance of HTS induction motor with HTS armature, the effect of n value on the electromagnetic torque is studied, as shown in Fig. 11. As can be seen from the figure, with the increase of n value, the electromagnetic torque decreases gradually, and the maximum electromagnetic torque tends to shift to the right. When the value of n is greater than 20, the

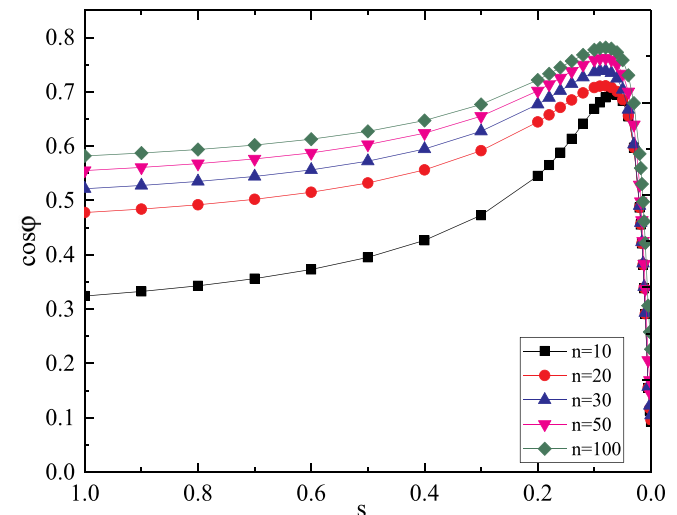


Fig. 10. Power factor vs slip rate under different n value of HTS tapes.

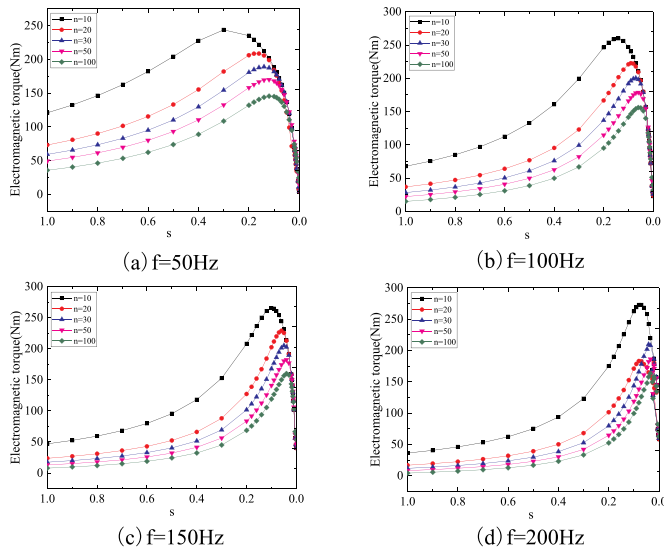


Fig. 11. Electromagnetic torque vs slip rate under different n value of HTS tapes.

electromagnetic torque presents clustering state. With the increase of frequency, the electromagnetic torque becomes steeper and steeper in the whole slip range, but the maximum electromagnetic torque remains almost unchanged. In addition, although the starting torque is too low, the motor can be started with the maximum torque by means of motor control strategy, which also makes up for the problems that may arise from the low starting torque of this kind of motor.

Fig. 12 shows the effect of the slip rate on electromagnetic torque of HTS induction motor with HTS armature under different critical current of superconducting tape. According to the figure, the electromagnetic torque increases with the increase of the critical current value of the superconducting tape, and the maximum electromagnetic torque value is also increasing. In addition, it can be seen that the maximum electromagnetic torque has a left-shift trend. On the other hand, it also shows that the range of adjustable speed of the motor is enlarged. When the critical current of the superconducting tape increases to a certain value, especially when the critical current is greater than 250A, the electromagnetic torque of the motor almost remains unchanged.

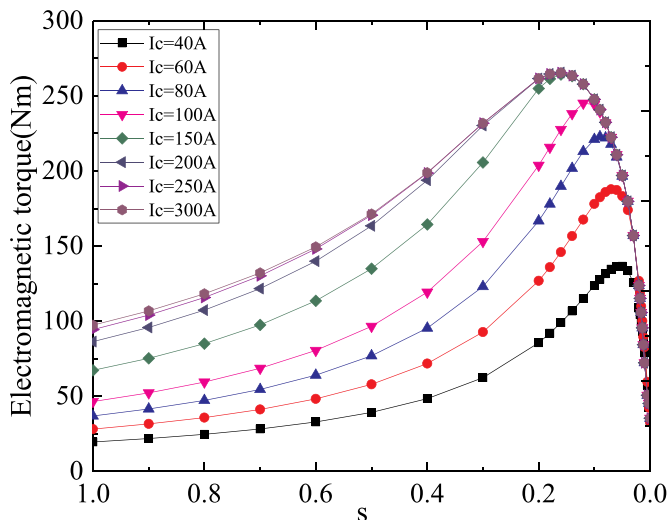


Fig. 12. Electromagnetic torque vs slip rate under different critical currents of HTS tapes.

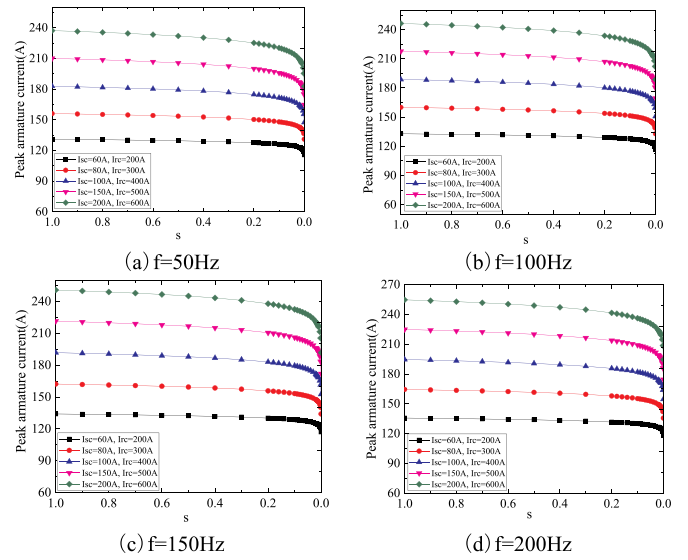


Fig. 13. Armature current vs slip rate under different critical currents.

3.3. LR circuit model of fully superconducting HTS induction motor

When the stator and rotor windings of the motor in the above two cases are all superconducting, it is a fully superconducting HTS induction motor. In this case, the resistance of stator and rotor is replaced by formula (20) and (22) in differential Eqs. (13) and (14) respectively. The other parameters of the motor remain unchanged and the cooling structure of the superconducting material in the motor is also neglected.

Fig. 13 is the variation curve between armature current peak value and slip rate of fully superconducting HTS induction motor under different critical currents and frequencies of superconducting tapes. As can be seen from the figure, when the frequency increases from 50Hz to 200Hz, the variation of armature current is very small and basically remains unchanged. When the critical current value of superconducting tape used in stator coil increases from 60A to 200A and the critical current value of rotor winding increases from 200A to 600A, the peak value of armature current increases continuously, and the armature current remains basically unchanged in a large range of motor operation. When the motor approaches the synchronous speed, the armature current peak has a tendency to gradually reduce, and it also conforms to the normal operation of the machine.

According to the analysis of the HTS induction motor with HTS rotor, the peak current of the rotor is always greater than the critical current, so it is necessary to analyze the influence of the rotor current. Fig. 14 shows variation curve of the ratio of peak rotor current to superconducting critical current and the slip ratio. It can be seen from the figure that the ratio of rotor current peak to critical current is too large for the fully superconducting HTS induction motor, and the maximum value is also close to 1.7 times. In addition, the rotor current is too large when the motor starts, even when the motor approaches the synchronous speed, the rotor current is only equal to the critical current.

The armature current of fully superconducting HTS induction motor is better than that of HTS induction motor with HTS armature, and the operation performance of the motor is also better. However, due to the problem that the rotor current is larger than the critical current, and the cost problem is aggravated by the use of HTS materials in both stator and rotor, the structure of HTS induction motor with HTS armature is finally adopted.

4. Conclusion

In this paper, the electromagnetic properties of HTS tapes are introduced from the perspective of the equivalent resistivity. The LR

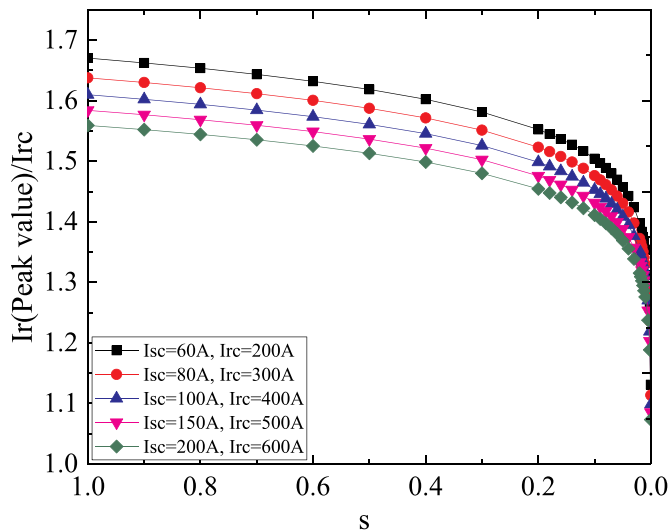


Fig. 14. Ratio of peak value of rotor current to critical current vs slip rate.

circuit model is studied from the aspect of whether superconducting materials are used in stator and rotor. The conclusions are as follows:

- (1) Superconductor has no resistivity when it is far below its critical current density, but it increases with the increase of the current density. The closer it approaches the critical current density, the more obvious the resistivity of superconductor is. With the increase of background magnetic field, the resistivity of superconductors is also increasing. When the background magnetic field exceeds a certain value, the resistivity of superconductors should be considered.
- (2) Based on the equivalent circuit model of traditional motor and the E-J rule of superconducting material, the ordinary differential equations of stator current and rotor current are derived. The differential equations are discretized by Euler method to solve ordinary differential equations. Finally, the discretization forms of stator current and rotor current of motor are obtained.
- (3) The LR circuit model is used to study HTS induction motor with HTS rotor, HTS induction motor with HTS armature and fully superconducting HTS induction motor. The results show that the HTS induction motor with HTS rotor and the fully superconducting HTS induction motor have wide speed range and large starting torque. However, the ratio of peak rotor current to critical current is greater than 1, and the stator current of HTS induction motor with HTS

armature remains almost unchanged in a large speed range, and there is no case that the armature current is higher than the critical current.

Declaration of Competing Interest

We declare that we have no financial and personal relationships with other people or organizations that can inappropriately influence our work.

References

- [1] S. Baik, Y. Kwon, Electrical design of a 17 MW class HTS motor for ship propulsion, *J. Supercond. Novel Magn.* 26 (4) (2013) 1283–1287.
- [2] S. Baik, et al., Performance Analysis of a Superconducting Motor for Higher Efficiency Design, *IEEE Trans. Appl. Supercond.* 23 (520200433) (2013).
- [3] G. Snitchler, B. Gamble, S.S. Kalsi, The performance of a 5 MW high temperature superconductor ship propulsion motor, *IEEE Trans. Appl. Supercond.* 15 (2) (2005) 2206–2209.
- [4] P.W. Eckels, G. Snitchler, 5 MW high temperature superconductor ship propulsion motor design and test results, *Nav. Eng. J.* 117 (4) (2005) 31–36.
- [5] J.H. Kim, et al., Analysis of the mechanical characteristics of a 17-MW-class high-temperature superconducting synchronous motor, *J. Supercond. Novel Magn.* 28 (2) (2015) 671–679.
- [6] P.J. Masson, J.E. Pienkos, C.A. Luongo, Scaling up of HTS motor based on trapped flux and flux concentration for large aircraft propulsion, *IEEE Trans. Appl. Supercond.* 17 (2) (2007) 1579–1582.
- [7] S. Lee, et al., Study on homopolar superconductivity synchronous motors for ship propulsion application, *IEEE Trans. Appl. Supercond.* 18 (2) (2008) 717–720.
- [8] E.H. Ailam, A. Hocine, M.N. Benallal, Comparison study between three kind superconducting motors, 2014 9TH International Electric Power Quality and Supply reliability Conference (PQ 2014), 2014, pp. 229–232.
- [9] C.Y. Cui, et al., Analysis of driving torque generated by superconducting motor based on the Meissner effect, 2015 IEEE International Conference on Applied Superconductivity and Electromagnetic Devices (ASEMD), (2015), pp. 439–440.
- [10] K. Tamura, et al., Study on the optimum arrangement of the field winding for a 20-kW fully superconducting motor, *IEEE Trans. Appl. Supercond.* 26 (4) (2016) 1–5.
- [11] S. Fukui, et al., Study of 10 MW-class wind turbine synchronous generators with HTS field windings, *IEEE Trans. Appl. Supercond.* 21 (32) (2011) 1151–1154.
- [12] K. Ikeda, et al., Hysteretic rotating characteristics of an HTS induction/synchronous motor, *IEEE Trans. Appl. Supercond.* 27 (4) (2017) 1–5.
- [13] W. Zhang, D. Xia, D. Zhang, Analysis of the strain and stress in the HTS generator at different operating conditions, *IEEE Trans. Appl. Supercond.* 27 (4) (2017) 1–5.
- [14] W. Zhang, D. Xia, D. Zhang, Parameter design by a novel method and optimization of the field coil for a 500 kW air-gap HTS generator, *IEEE Trans. Appl. Supercond.* 24 (3) (2013) 1–4.
- [15] H. Lim, et al., AC losses of pancake winding and solenoidal winding made of YBCO wire for superconducting transformers, *IEEE Trans. Appl. Supercond.* 17 (2) (2007) 1951–1954.
- [16] M. Fratila, et al., Iron loss calculation in a synchronous generator using finite element analysis, *IEEE Trans. Energy Convers.* 32 (2) (2017) 640–648.
- [17] P.J. Masson, et al., Development of a 3D sizing model for all-superconducting machines for turbo-electric aircraft propulsion, *IEEE Trans. Appl. Supercond.* 23 (3) (2013) 3600805.